Visual Neuroscience (1994), **11**, 619–628. Printed in the USA.

Receptor demise from alteration of glycosylation site in *Drosophila* opsin: Electrophysiology, microspectrophotometry, and electron microscopy

GARY BROWN,[1] DE-MAO CHEN,[1] J. SCOTT CHRISTIANSON,[2] RON LEE,[1] AND WILLIAM S. STARK[1]

[1]Department of Biology, Saint Louis University, Missouri
[2]Mason Institute of Ophthalmology, University of Missouri, Columbia

(RECEIVED September 7, 1993; ACCEPTED December 3, 1993)

Abstract

In the ΔAsn_{20} *Drosophila* stock, the N-linked glycosylation site of opsin in R1-6 receptors (Rh1) is absent. We used electroretinography (ERG), microspectrophotometry (MSP), and electron microscopy (EM) to quantify visual cell defects. Positive controls, *w9*, had wild type Rh1. MSP revealed minimal photopigment in ΔAsn_{20} for 6 days posteclosion; *w9* had near normal visual pigment. ERG sensitivity and prolonged depolarizing afterpotential (PDA) were compared for ΔAsn_{20} and *w9*. ΔAsn_{20}'s R1-6 function is decreased 100-fold at eclosion and diminishes until only R7/8 functions at 11 days. What little rhodopsin is routed to the rhabdomere functions. Morphometry showed smaller R1-6 rhabdomeres in ΔAsn_{20} for 8 days posteclosion. Rhabdomeres in *w9* were normal. A negative control, $ninaE^{ol17}$, a deletion of the Rh1 gene, also has small rhabdomeres. ΔAsn_{20} and $ninaE^{ol17}$ lack the extreme rhabdomere elimination of *ora* (*o*uter *r*habdomeres *a*bsent), a nonsense mutant interrupting Rh1's coding sequence. ΔAsn_{20} and *ora* have surplus membrane while $ninaE^{ol17}$ does not. Freeze fracture reveals that ΔAsn_{20}'s rhabdomeric P-face particle count is as low as for vitamin A deprivation, consistent with an opsin defect. High particle density, organized into rows, is present in adjacent plasmalemma where surplus membrane accumulates. In summary, ΔAsn_{20} interferes with either synthesis, deployment, or maintenance of opsin.

Keywords: Glycosylation, *Drosophila*, Morphometry, Rhodopsin, Mutant, Sensitivity, Endoplasmic reticulum

Introduction

Packing opsin into membranes of microvillar organelles, called rhabdomeres in *Drosophila* photoreceptors, requires well-orchestrated protein synthesis and routing. Like many membrane proteins, opsin undergoes N-linked glycosylation cotranslationally in the rough endoplasmic reticulum. Huber et al. (1990) showed that newly synthesized *Calliphora* opsin is glycosylated while mature rhabdomeric rhodopsin is not (see also Ozaki et al., 1993). This confirms and extends an earlier report (deCouet & Tanimura, 1987) that *Drosophila* rhodopsin is not glycosylated. Tunicamycin has been used to inhibit glycosylation since it blocks the biosynthesis of N-linked oligosaccharides attached to glycoproteins (reviewed by Elbein, 1987). In *Drosophila*, tunicamycin blocks rhodopsin recovery by carotenoid replacement in vitamin A deprived flies (Stark et al., 1991), implicating that glycosylation is pivotal in opsin traffic.

In the vertebrate, rhodopsin need not be glycosylated in order to function in phototransduction since the spectrum and regenerability of bovine opsin are not altered by enzymatic deglycosylation (Krishna Prasad et al., 1992). However, glycosylation may influence opsin routing into the outer segment. In *Xenopus laevis* and *Rana pipiens* retinas, tunicamycin blocks glycosylation and disrupts disc membrane assembly, eventually causing retinal degeneration (Fliesler & Basinger, 1985; Fliesler et al., 1984, 1985).

In this study, we examined the cell biology of rhodopsin deployment and function by taking advantage of a glycosylation deficient *Drosophila* mutant. O'Tousa (1992) transfected the germline of an opsin deletion, $ninaE^{ol17}$, with a coding sequence in which the N-linked glycosylation site was altered. In the resulting strain, dubbed ΔAsn_{20}, the asparagine (N = Asn) residue at position #20 of the opsin protein was replaced by isoleucine (Ile, a codon change of AAT to ATT). Ile was cho-

Reprint requests to: William S. Stark, Department of Biology, Saint Louis University, 3705 Laclede Avenue, Saint Louis, MO 63103-2010, USA.

sen as an appropriate substitute for Asn because it contains a nonreactive carbon side group. ΔAsn_{20} flies had normal steady-state mRNA levels as assessed by Northern blots, but much lower rhodopsin levels (measured with protein gels). This means that transcription is not at fault. Positive controls, *w9*, were opsin deletions transformed with the wild type Rh1 gene (O'Tousa, 1992). We extended O'Tousa's initial description on ΔAsn_{20} by quantifying visual pigment, sensitivity, rhabdomere area, and the cellular ultrastructure. An abstract of these findings has already been published (Chen et al., 1992*a*).

Methods

Animals

Drosophila melanogaster were raised on a standard medium with enough carotenoids for fully developed visual function (Chen et al., 1992*b*; Stark et al., 1990). Sources of carotenoids in the medium were yellow cornmeal and a supplementation of β-carotene at 0.125 mg/ml, the minimum dose found to maximize sensitivity (Stark et al., 1977) and visual pigment (Stark & Johnson, 1980; Stark et al., 1990) for flies reared from egg to adult on an otherwise carotenoid-deficient medium. Flies were reared in a 12-h light/12-h dark (L/D) cycle of laboratory fluorescent (Phillips 30-W Cool White) lighting at an intensity of 75–80 lux (Lutron LX 101 digital lux meter).

Stocks of white-eyed ΔAsn_{20}, *w9*, and $ninaE^{ol17}$ were obtained from Professor Joe O'Tousa at Notre Dame University. ΔAsn_{20} and *w9* resulted from his recent work (O'Tousa, 1992) while $ninaE^{ol17}$ was described earlier (O'Tousa et al., 1985). Originally, O'Tousa (1992) showed similar deficits in two independent isolates with different sites of incorporation of the gene into the genome: ΔAsn_{20} #2 and #4. All of the work reported here utilized #4. $ninaE^{ol17}$ is a large deletion encompassing most of the opsin gene and a large upstream region. As the deletion strain was used as a parental strain of both normal and ΔAsn_{20} opsin genes, it would seem to be an appropriate control for the observations made on these transformants. We report our *ol17* data, but with the following caveat. The two *ol17* lines provided to us by O'Tousa and bearing different markers had different ERG phenotypes. One, marked with *ry*, had an ERG as expected from R7 and R8 (Britt et al., 1993). The other, marked with *sr*, had considerable R1-6 function even to 4 days posteclosion. Both had diminished rhabdomeres and other ultrastructural features suggestive of abnormality. Our data is from the *ry* strain (although we also present data from the *sr* strain in Fig. 1).

The lack of eye color in white-eyed constructs allowed for visual pigment and sensitivity determinations unconfounded by the spectral effects of screening pigments.

Deep pseudopupil microspectrophotometry

Our techniques for measuring visual pigment from R1-6 rhabdomeres of live *Drosophila* have been previously described (Sapp et al., 1991; Stark & Johnson, 1980). The measurement is based on the nonbleaching photointerconversion of a 480-nm absorbing rhodopsin with its 570-nm absorbing metarhodopsin. The deep pseudopupil was viewed with 579-nm light, at the absorbance difference spectrum's maximum. This image was localized into a closely fitting aperture in front of a photomultiplier. Maximal rhodopsin was created by applying a 620-nm stimulus for 10 s at 16.2 log quanta/cm^2·s. Then transmission of 579-nm light through the deep pseudopupil was measured. Metarhodopsin was subsequently maximized by applying 450-nm light at 15.8 log quanta/cm^2·s for 10 s. The transmission was again measured. The log of the ratio of these two transmissions (after 620 nm *vs.* after 450 nm) is the absorbance difference.

Electroretinography

ERGs were recorded using refinements of previously described methods (e.g. Chen et al., 1992*b*; Stark & Wasserman, 1972). The fly's compound eye was carefully located at the focal plane of an optical stimulator using 625-nm light at an intensity of 16.3 quanta/cm^2·s. A glass micropipette was inserted into the

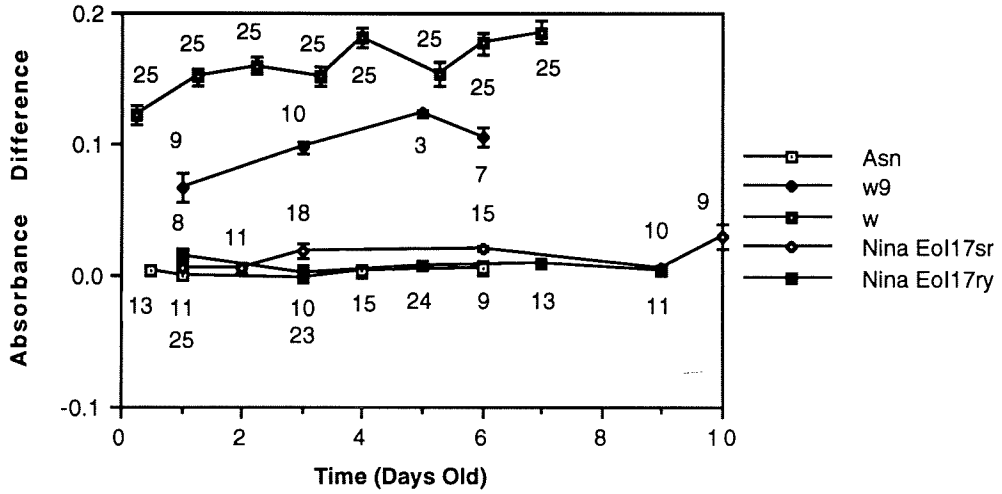

Fig. 1. Microspectrophotometry of ΔAsn_{20}, $ninaE^{ol17}$ (two strains, one selected with *sr* and the other with *ry* as markers, the negative controls) *w9* (the positive control). Average absorbance difference as a function of days posteclosion is plotted ($n \pm$ S.E.). For comparison, the data from a normal white-eyed positive control strain is replotted from an earlier study (Zinkl et al., 1990).

retinal cell layer. The fly was dark adapted for 40 min before collecting the dark-adapted spectral sensitivity for a 2-mV peak-to-peak criterion potential. The prolonged depolarizing afterpotential (PDA) was induced by 470-nm stimulation at about 16.2 log quanta/cm^2·s for 2 s and was reversed by 570-nm stimulation at about 16.3 log quanta/cm^2·s for 2 s.

Electron microscopy (EM) and morphometry

We fixed fly heads for transmission EM and subsequent morphometry using aldehyde prefix, osmium postfix, and lead and uranyl staining as previously published (e.g. Chen et al., 1992*b*; Stark & Clark, 1973). Although xylene had been used in some earlier studies (e.g. Stark & Sapp, 1987) to expand sections while they were in the boat of the diamond knife, this step was omitted to avoid variability in our morphometric measurements. For morphometry, sections were photographed at 7500× on a JEOL 1200 transmission TM. Because the rhabdomeres taper slightly, photographs were always taken at one plane in the distal-proximal extent, specifically the R1-6 nuclear layer where most ommatidia sampled showed at least two nuclei. For further control, we only photographed sagitally sectioned heads with well cross-sectioned rhabdomeres near the equator.

Morphometric measurements were accomplished on our computer digitized image analysis system (Chen et al., 1992*b*; Katz et al., 1991; Sapp et al., 1991; Stark et al., 1991; Zinkl et al., 1990). We focussed a Dage MTI CCD-72 video camera (with a Fujicon HF35A-2 lens) onto EM negatives using an Aristo DA-10 light box. Images were fed into an AIC (Analytical Imaging Concepts) model IM morphometric and densitometric system operated on a Northgate 286 computer. Rhabdomere perimeters were manually traced to obtain a measurement of cross-sectional area.

Freeze-fracture electron microscopy

Freeze-fracture EM was performed as previously described (Stark & Carlson, 1983; Stark et al., 1987, 1989; Stark & Sapp, 1988) with modifications (Katz et al., 1991). Heads were dissected in a fixative consisting of 1% gluteraldehyde, 0.17 M sodium cacodylate, pH = 7.4 at room temperature for at least 20 min. After an initial period of fixation to harden the retina somewhat, heads were sliced into smaller fragments so that they could be packed onto the hat-shaped specimen holder for the fracture apparatus. Specimens were washed in 0.17 M sodium cacodylate, pH = 7.4 and then were placed into a vial containing 4 ml of this buffer. Glycerol was slowly added to the vials over a 2-h period until a final concentration of 30% of this cryoprotectorant was achieved.

Heads were packed onto gold specimen holders using a holding paste of live yeast growing in the glycerinated buffer. Holders were quickly frozen in liquid freon (cooled by liquid nitrogen) and stored in liquid nitrogen. Frozen samples were fractured at −102°C by razor under visual control, and plated with platinum and carbon in the Bendix-Balzers 301 freeze-fracture apparatus. The holders were immersed in chromic acid–sulfuric acid for 1–2 days, and the replicas were transferred to a distilled water wash with the aid of copper grids. Replicas were then mounted on uncoated copper grids which had been soaked briefly in an azure blue solution (about 0.1 mg/ml) and viewed and photographed on a JEOL CX Transmission EM. The AIC morphometric computer was used to facilitate quantification of P-face particles. Identification of particles in freeze-fracture electron microscopy has always been subjective, but this is less of a problem for low counts such as those we present.

Results

Microspectrophotometry (MSP)

MSP revealed that ΔAsn_{20} and $ninaE^{ol17}$ flies have little visual pigment within a week after eclosion (Fig. 1). The positive *w9* controls had much higher visual pigment than ΔAsn_{20} and $ninaE^{ol17}$. We consider visual pigment in *w9* to be near normal, although it is slightly lower than for white-eyed otherwise wild-type flies [data from Zinkl et al. (1990)].

Electrophysiology

Three aspects of the ERG can be used to infer R1-6 function and health: the prolonged depolarizing afterpotential (PDA), the ON and OFF transients, and the sensitivity. The PDA is a "locking in" of the R1-6 receptor potential (e.g. Stark et al., 1976). The ON and OFF transients are from R1-6 synapses in the lamina (e.g. Shaw, 1981). Fig. 2 shows both of these measurements at 1, 5, 7, and 11 days after eclosion. The PDA of ΔAsn_{20} at 1 and 5 days is small and witnessed only as a slow return to baseline after 470-nm stimulation. The PDA is diminished at 7 days. At 11 days postemergence, ΔAsn_{20} flies no longer exhibit any PDA. Thus, there is a reduction of R1-6 function with the end result being an ERG which looks like that for R7/8 alone (Stark & Zitzmann, 1976).

The ON and OFF transients of the ERG follow the same pattern as the PDA: small for newly eclosed and diminishing with age until, at 11 days, the ON and OFF transients are gone. Again, this points to a demise in R1-6 receptor function with age in ΔAsn_{20}. Fig. 3 shows the presence of normal PDA and ERG transients for the positive controls, *w9*, at 7 days.

ERG sensitivity measurements were used to quantify ΔAsn_{20}'s loss of R1-6 function from the newly eclosed level to the point at which only R7/8 function could be detected (Fig. 4); *w9*'s sensitivity starts out and remains at the expected high control levels. Sensitivity was determined at 470 nm for *w9* and ΔAsn_{20} as a function of age posteclosion to 11 days. ΔAsn_{20} flies start out 2 log units less sensitive than *w9*, and the sensitivity decreases with age for ΔAsn_{20} flies.

Fig. 5 expands on this finding by presenting entire spectral sensitivities at selected ages. For the positive control, *w9*, the spectral sensitivity stays constant and resembles that widely published for R1-6 (e.g. Harris et al., 1976). For ΔAsn_{20} flies, in the UV region of the spectrum (where R7 sensitivity is high), the sensitivity does not decrease with age. However, in the visible region (>400 nm) the sensitivity decreases almost 1 full log unit from $\frac{1}{2}$ day to 11 days. Considered in light of the relative levels and shapes of the R1-6 *vs.* R7/8 spectra (Harris et al., 1976), the data of Figs. 4 and 5 can be interpreted as follows: (1) R1-6 function is diminished 100-fold in newly emerged ΔAsn_{20} flies; and (2) the remaining function is eventually lost, leaving only R7/8 functional in the compound eye's ERG.

Fig. 6 shows the ERG intensity–response functions at selected ages in ΔAsn_{20}. At 1 day, the receptor potential reaches 25 mV at a saturating intensity level, a substantial fraction of that expected for normal flies and about that obtained from vitamin A deprived flies (Stark et al., 1991). Later, the intensity–

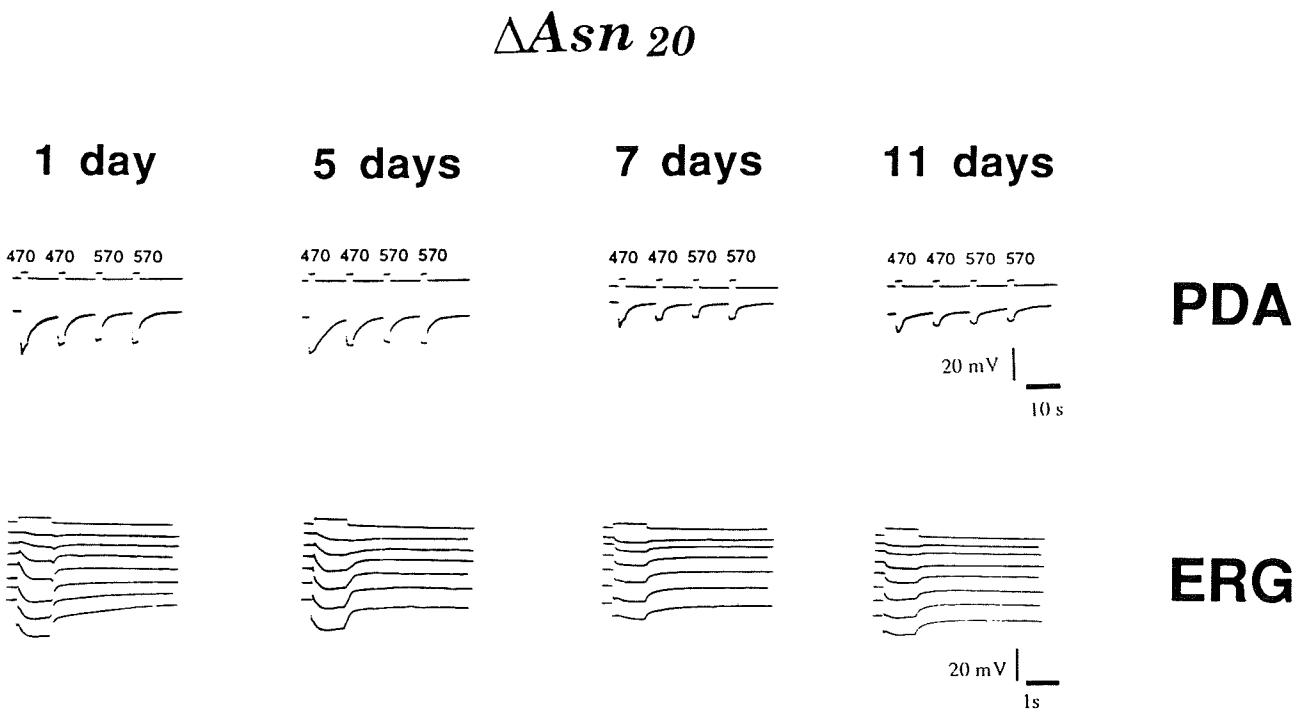

Fig. 2. ERG waveforms from ΔAsn_{20} flies at 1, 5, 7, and 11 days. The top of the figure, labeled "PDA," shows responses (lower tracings) on a slow time scale to intense 470- and 570-nm stimuli (upward deflections on upper tracings, 16.09 and 16.32 log {quanta/cm^2·s}, respectively) to demonstrate the PDA (prolonged depolarizing afterpotential) properties. Larger responses to all stimuli at 1 day (also 5 days) and slow repolarizations after 470-nm stimuli demonstrate minimal R1-6 function and PDA's, respectively. The responsivity at 7 and 11 days is that of the compound eye with only R7/8 functional (e.g. Harris & Stark, 1977; Harris et al., 1976). The bottom of the figure, labeled "ERG," shows faster sweep speeds for intensity–responsivity series of ERG waveforms elicited by 470-nm stimuli (upward deflections on the top most tracings). The intensity ranges are as follows: 9.7 (second tracing from top) to 14.6 (bottom tracing, intensities in log quantum flux as above) at 1 day, 10.6 to 14.2 at 5 days, 11.3 to 15.1 at 7 days, and 11.3 to 16.2 at 11 days. The diminishing ON and OFF transients and responses, as well as the higher stimuli needed to obtain the responses, indicate an early R1-6 function which disappears (leaving only R7/8 functional) with age. Calibration axes show gains and sweep speeds for both PDA and ERG experiments.

response function better resembles that obtained when only R7/8 are functional in the compound eye (e.g. Stark & Zitzmann, 1976).

Electron microscopy

Fig. 7 shows the R1-6 cross-sectional area as measured by computerized image analysis from EM. ΔAsn_{20} flies have small R1-6 rhabdomeres at emergence which may decrease a small amount with age. ΔAsn_{20} rhabdomeres are about half of the size of the rhabdomeres in *w9* [which approximate those of wild type (Chen et al., 1992*b*; Sapp et al., 1991)]. $ninaE^{ol17}$ have small rhabdomeres like those of ΔAsn_{20} flies and much smaller than those of *w9*. Importantly, both ΔAsn_{20} and *w9* still have R1-6 rhabdomeres at 1 week. By contrast, micrographs from $ninaE^{ora}$ flies (see Discussion) suggest that the R1-6 rhabdomeres are largely gone by 1 week (O'Tousa et al., 1989; Stark & Sapp, 1987). In all three strains, R7 rhabdomeres served as an internal control since they express different opsin genes. R7 area does not differ with age in ΔAsn_{20}, *w9*, or $ninaE^{ol17}$ (Fig. 8). These values are also close to those previously obtained for wild type (Chen et al., 1992*b*; Sapp et al., 1991).

Cross-sectioned ommatidia of *w9* (Figs. 9 and 10) and ΔAsn_{20} (Figs. 11 and 12) are shown. In 1-day-old *w9* (Fig. 9), rhabdomere size is normal, and it appears that normal cycling of photomembrane is occurring, as indicated by the multivesicular bodies (MVBs). At 8 days, *w9* still appears healthy (Fig. 10). ΔAsn_{20}, however, has small R1-6 rhabdomeres at 1 day (Fig. 11). Occasionally, the belt desmosomes which join retinula cells, normally situated right at the intraommatidial cavity (cf. Figs. 9 and 10), are slightly recessed. At 8 days (Fig. 12), ΔAsn_{20}'s rhabdomeres are still small (note that one R1-6 rhabdomere has almost disappeared). Also membrane specializations with a zipper-like appearance (Alawi et al., 1972; Stark & Sapp, 1989; Stark et al., 1989) have developed between the belt desmosome and the intraommatidial cavity. R7 cells are about the same size in all micrographs.

Fig. 13 shows that $ninaE^{ol17}$ has diminished rhabdomeres at 3 days posteclosion but does not have zipper-like membrane accumulations. Although Leonard et al.'s (1992) micrograph of white-eyed $ninaE^{ol17}$ aged 1 week showed slightly smaller rhabdomeres, we consider the findings to be the same. Neither study showed cellular degeneration, witnessed by electron densification.

Fig. 14 shows a freeze-fracture electron micrograph of ΔAsn_{20} showing that there are very few P-face particles in the

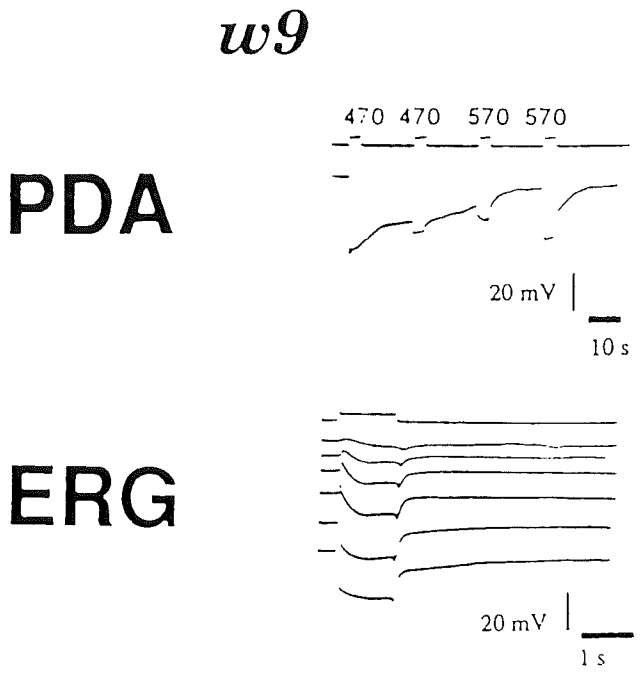

Fig. 3. PDA and ERG properties obtained from *w9* at 7 days posteclosion. The presentation is as in Fig. 2. For the PDA, intensities are 16.2 log quantum flux at 470 nm and 16.4 at 570 nm. For the ERG, the intensity range is 8.4 to 12.2. Note the much more sustained corneal negativity after 470-nm stimulation (downward deflection) which is repolarized after actinic light at 570 nm in the PDA experiment. This more closely matches the tracings for normal flies with R1-6 functional (e.g. Stark & Zitzmann, 1976). Also, the presence of ON and OFF transients and the high sensitivity (low intensities needed to elicit the ERG's shown on the bottom of the figure) are indicative of normal R1-6 function.

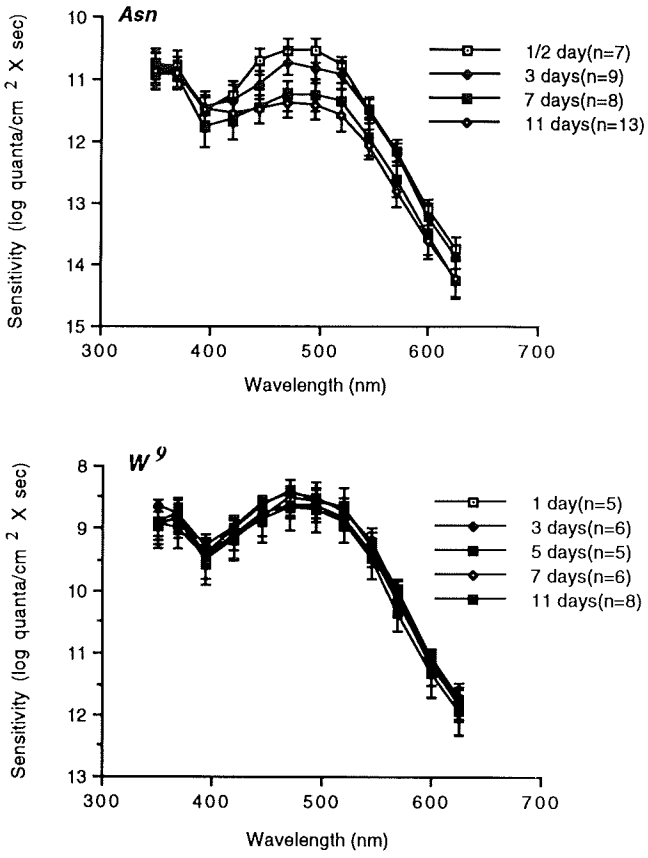

Fig. 5. Spectral sensitivity for the ERG of *w9* and ΔAsn_{20} flies at selected ages to 11 days. Criterion, intensity units, and averaging are as in Fig. 4.

rhabdomeric microvilli, a picture much like that obtained from vitamin A deprived flies. Note that we were fortunate to obtain a fracture plane which included the plasmalemma adjacent to the microvilli, and this membrane reflects the particle density of the microvilli out to a point. Beyond that point, high density and ridges mark the probable location of the zipper-like membrane specialization. Counts of P-face particle density were as follows: rhabdomeric microvilli -1000 ± 60 (S.E.)/μm^2, close adjacent area $-1010 \pm 12/\mu m^2$, and area of higher density $-3953 \pm 84/\mu m^2$.

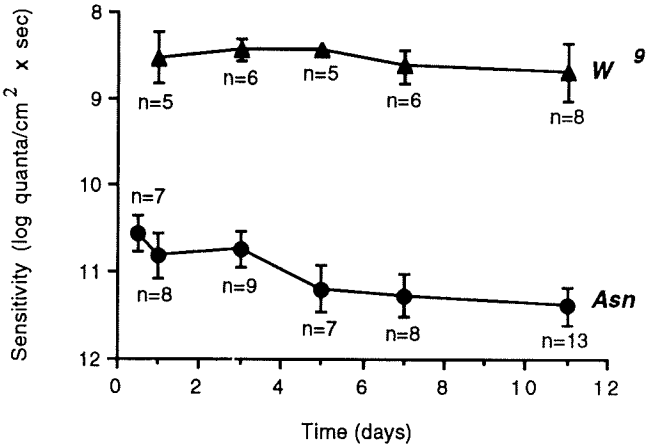

Fig. 4. ERG sensitivity as a function of adult age posteclosion for *w9* and ΔAsn_{20} flies assayed at 470 nm. Sensitivity was determined as inverse log intensity [quanta/cm^2·s] for a 2-mV peak-to-peak ERG and was averaged from the number of preparations shown with the S.E. as a vertical bar.

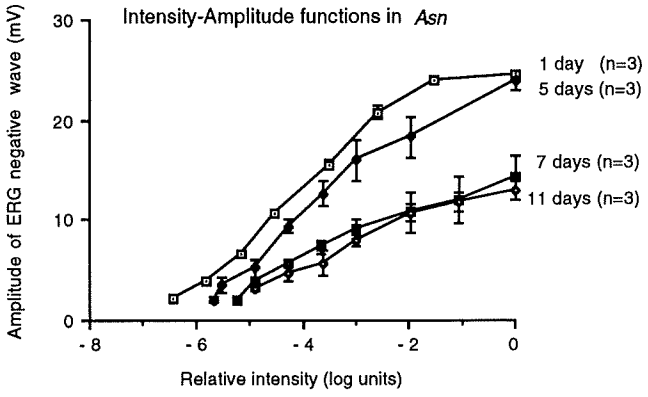

Fig. 6. Intensity–response function for the negative wave (receptor potential) of the ERG at selected ages posteclosion. Amplitude (mV) is plotted as a function of relative intensity (log quantum flux) where 0 corresponds with 16.12 ± 0.04 log quanta/cm^2·s. Numbers of preparations averaged and standard errors are shown.

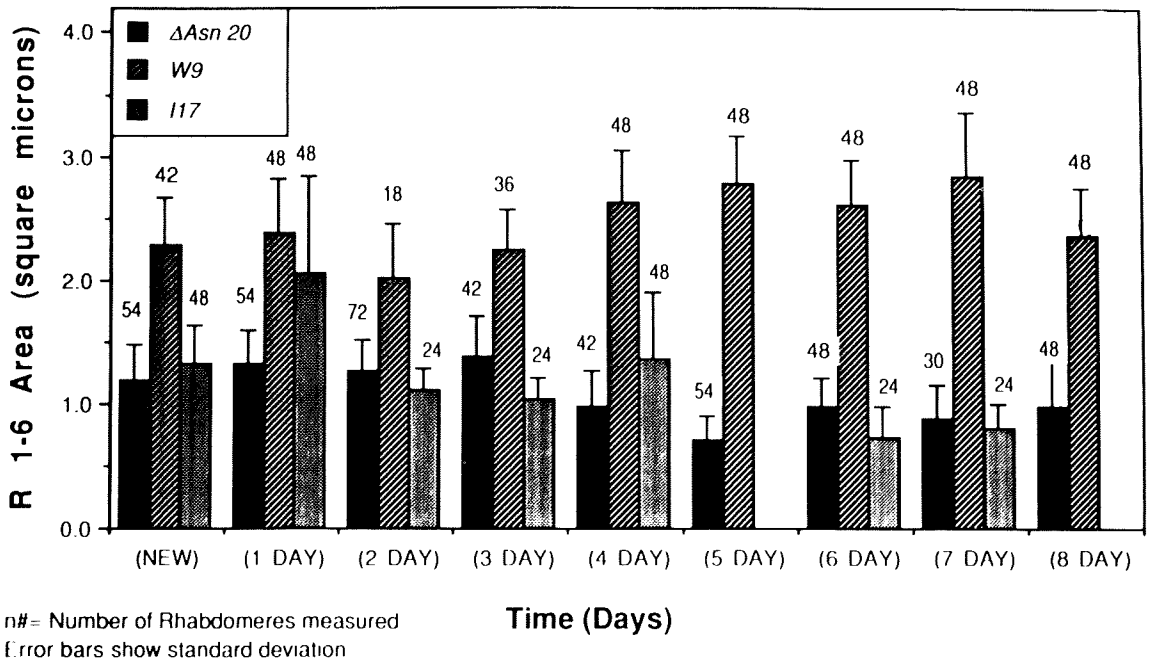

Fig. 7. Rhabdomere area of R1-6 determined by computerized morphometric analysis over a 9-day period is shown for ΔAsn_{20}, *w9*, and $ninaE^{o117}$. Numbers above the error bars represent the number of rhabdomeres measured. Error bars show the standard deviation.

Discussion

Our results suggest that ΔAsn_{20} interferes with either the synthesis, deployment, or maintenance of rhodopsin, but not its phototransduction function. For instance, synthesis could theoretically be abnormal, but transcription is not: opsin mRNA level in ΔAsn_{20} is not different from that of wild type (O'Tousa, 1992). On the other hand, our evidence favors incorrect deploy-

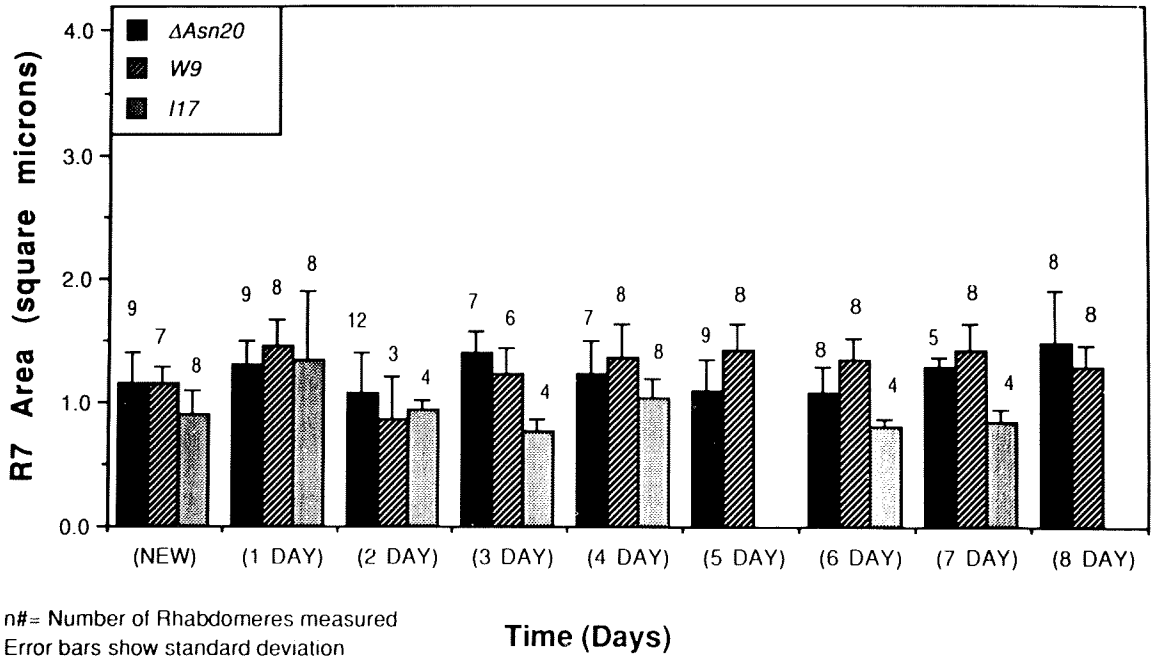

Fig. 8. Rhabdomere area of R7 determined by computerized morphometric analysis over a 9-day period is shown for ΔAsn_{20}, *w9*, and $ninaE^{o117}$. Numbers above the error bars represent the number of rhabdomeres measured. Error bars show the standard deviation.

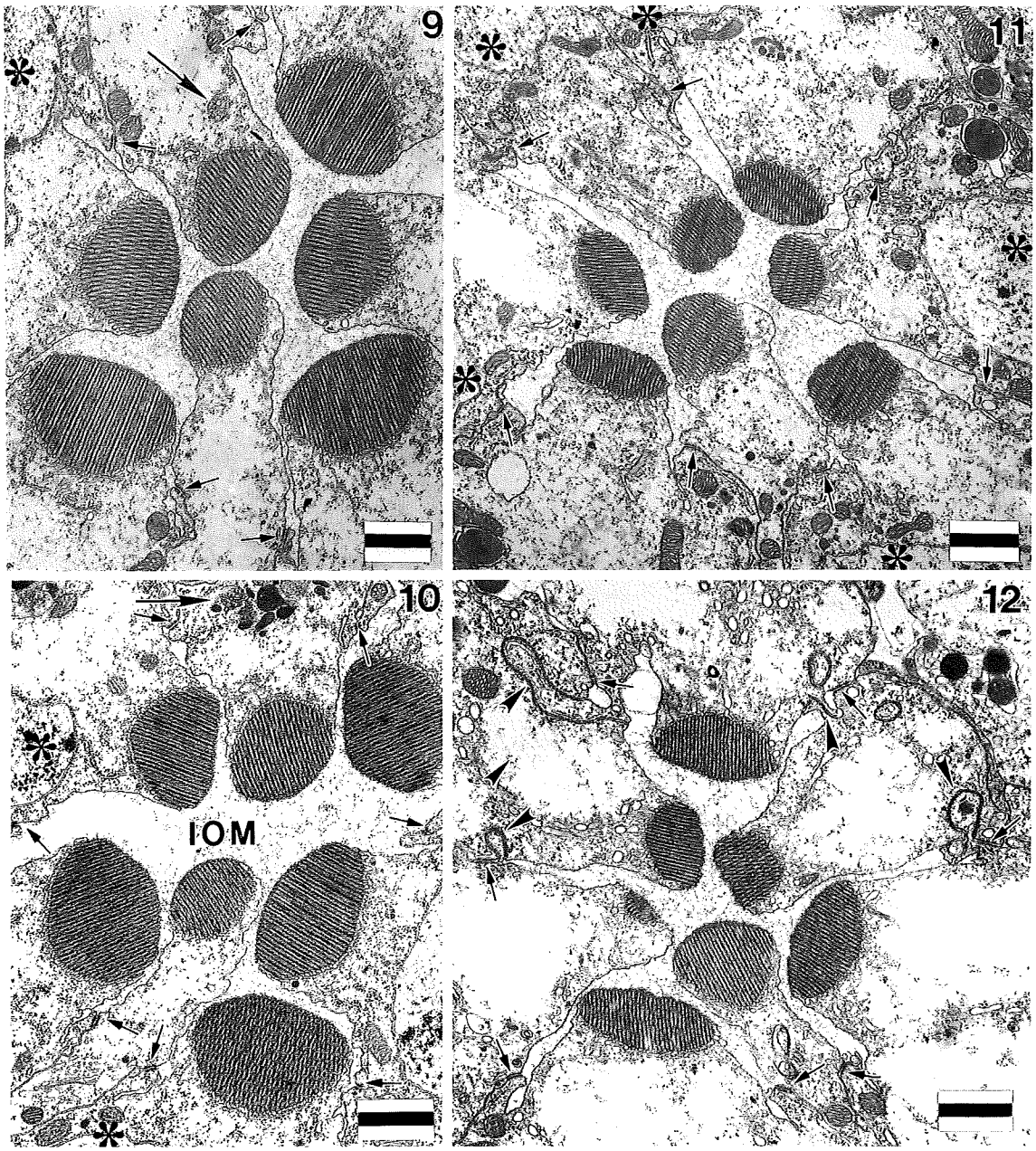

Figs. 9–12. Cross-sectioned ommatidia at the levels of the R1-6 nuclei [*] of *w9* (Figs. 9 and 10) and ΔAsn_{20} (Figs. 11 and 12) on the first day after eclosion (Figs. 9 and 11) and 8 days after eclosion (Figs. 10 and 12). The intraommatidial cavity (IOM) is central in each micrograph, and R7 inserts from the 6, 7, 6, and 5 o'clock positions in Figs. 9–12, respectively. Long arrows show MVB's seen in *w9* but not ΔAsn_{20}. Small arrows depict the belt desmosomes which are in the fields, normal in *w9*, sometimes recessed in 1-day ΔAsn_{20} and sometimes peripheral to the IOM by zipper-like membrane densities (arrowheads) in 8-day ΔAsn_{20}. Calibration bars = 1 μm.

ment or maintenance since R1-6 are partly functional. Possibly, a small amount of nonglycosylated rhodopsin leaks to the rhabdomere where it functions since normal rhabdomeric rhodopsin is not glycosylated (deCouet & Tanimura, 1987; Huber et al., 1990).

Many types of retinal dystrophies are caused by incorrect assembly and routing of opsin. An interesting example is in mutants of the *Drosophila ninaA* gene, in which a cyclophilin homolog is missing; this enzyme is required for proper protein folding by catalyzing peptidyl-prolyl *cis* to *trans* isomerization (Stamnes et al., 1992). In *ninaA* mutants, Rh1 is produced, but is not correctly routed to the rhabdomere; opsin accumulates in cisternae of the rough endoplasmic reticulum (Colley et al., 1991).

It is not surprising that visual pigment for ΔAsn_{20} and $ninaE^{ol17}$ is undetectable (Fig. 1). Beyond the scope of this MSP measurement, the ERG offers a log scale to quantify the minimal R1-6 function in newly emerged ΔAsn_{20} (Figs. 2 and

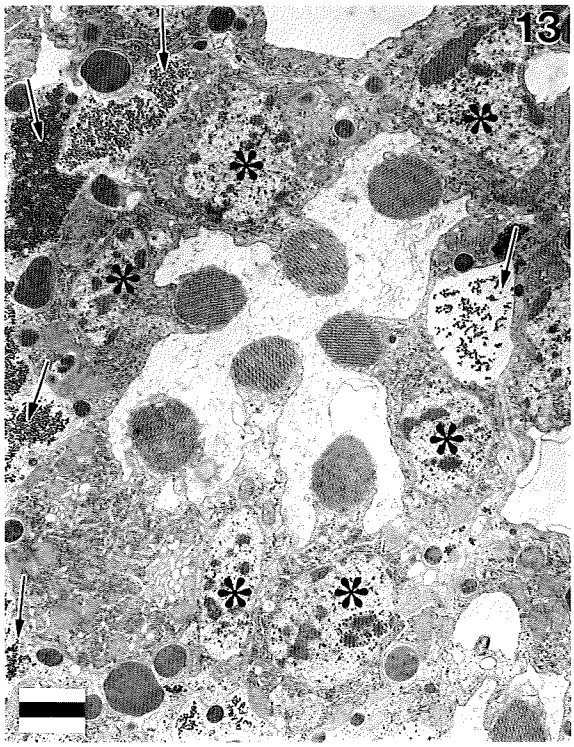

Fig. 13. A cross section of an ommatidium of the *ninaE*^{o117} stock marked with *ry* and aged 3 days. Note the absence of any of the zipper-like membrane specializations as seen in Fig. 12 for ΔAsn_{20}. R1-6 (numbered counterclockwise) are as small as R7 (inserting from the 6 o'clock position) in this cross section and much smaller than in *w9* as shown in Figs. 9 and 11. Nuclei [*] of R1-5 and R7 are shown. Retinula cell cytoplasm is dense with rough endoplasmic reticulum. Denser reticulum (arrows) is in the secondary pigment cells. Calibration bar = 1 μm.

4–6). We conclude that functional rhodopsin is reduced over 100-fold, although that which does "leak" to visual membranes mediates phototransduction. This is consistent with the finding in the vertebrate that spectrum and regenerability of rhodopsin do not require glycosylation (Krishna Prasad et al., 1992).

Interestingly, ΔAsn_{20} flies have surplus membrane between the belt desmosomes of retinula cells and the intraommatidial cavity. These unusual elaborations look like septate desmosomes and also like the "zippers" of the *no r*eceptor *p*otential mutant (Alawi et al., 1972; Stark & Sapp, 1989; Stark et al., 1989). The *Drosophila* mutant *o*uter *r*habdomeres *a*bsent (*ora*) also has such membranes (Stark & Sapp, 1987); *ora* is an allele of *ninaE* (the R1-6 opsin gene, see also below), hence the name *ninaE*^{ora} (Washburn & O'Tousa, 1992). The site of zipper accumulation is directly confluent with rhabdomeric microvilli (Stark et al., 1992). Thus, the abnormality could reflect a defect of opsin deployment which results in a "storage disease." The issue is unresolved, however, since the micrographs of Leonard et al. (1992) of several EMS-induced mutant alleles of *ninaE*, namely *P318*, *P332*, *P334*, and *P352*, did not show such membranes; since all these stocks were on a red-eyed background and the *ninaE*^{ora} vistas were from a white-eyed background, it is possible that lack of eye color pigmentation influences this abnormality. We were fortunate to obtain a freeze-fracture replica

Fig. 14. A freeze-fracture micrograph of ΔAsn_{20} showing the paucity of P-face particles in the rhabdomeric microvilli (M) and the adjacent plasmalemma (P). Beyond a certain distance (arrow) from the microvilli, the plasmalemma shows a higher P-face particle density with some particles organized into distinct ridges (arrowheads). We propose that this is a freeze-fracture visualization of the zipper-like membrane. Note the pock mark in the adjacent plasmalemma, the apparent site of a coated pit. Magnification = 29,000×.

which is almost certainly through the zipper. This vista is of considerable interest since it is the first view of its kind. It shows a high P-face particle density and a set of organized ridges.

The zipper is lacking, and rhabdomeres survive in $ninaE^{ol17}$ while $ninaE^{ora}$ has zippers. Also, in $ninaE^{ora}$, a nonsense mutation interrupting *Drosophila*'s opsin coding sequence at position 251 (Washburn & O'Tousa, 1992), rhabdomeres form and then diminish (O'Tousa et al., 1989; Stark & Sapp, 1987). The glycosylation deficient ΔAsn_{20} has zippers. These comparisons suggest that cells have less severe pathology with the opsin gene deletion than with improperly synthesized or routed opsin. We characterize $ninaE^{ol17}$ at the cell biological level since it was the strain used to construct the ΔAsn_{20} and *w9* lines. Our findings do not contradict the use of $ninaE^{ol17}$ in a number of other studies (e.g. Britt et al., 1993; Colley et al., 1991). We find the amount of rough endoplasmic reticulum in $ninaE^{ol17}$ to be curiously high considering that translation of opsin, the photoreceptor's predominant protein, should not even be initiated. Perhaps there is a compensatory increase in the translation of other proteins.

Mutations of opsin are becoming increasingly relevant. For instance, in the human, some forms of autosomal dominant retinitis pigmentosa are caused by single missense mutations in the opsin coding sequence (Dryja et al., 1990). By contrast, nonsense mutations should have gross effects, and one patient was blind from birth because of a stop codon at 249 (Rosenfeld et al., 1992). Since $ninaE^{ora}$ and human sites are nearly identical, it is interesting that heterozygous relatives of this affected patient and heterozygotes of $ninaE^{ora}$ (Chen et al., 1993) are both approximately 0.5 log units less sensitive than homozygous normals (Rosenfeld et al., 1992).

The present analyses of a missense mutation at a particularly important site in the opsin sequence thus integrates into a growing body of basic and clinical evidence concerning the proper function of the opsin gene.

Acknowledgments

Supported by NIH Grant RO1 EY07192. Part of the cost of maintaining one electron microscope facility was defrayed by a Research to Prevent Blindness grant to the Department of Ophthalmology at the University of Missouri—Columbia, and we thank Mr. Michael Norberg who supervised this facility during our studies. We thank Dr. Nancy Galvin of the Pathology Department at Saint Louis University who supervised the JEOL CX facility. We thank Professor Steven J. Fliesler of the Ophthalmology Department at Saint Louis University for comments on the manuscript and Professor Joe O'Tousa of the Biology Department at Notre Dame University for providing the *Drosophila* stocks. We thank Ms. Linnette Maier for initiating MSP experiments. We also thank Mr. Darren Hombs for his work in the darkroom.

References

Alawi, A.A., Jennings, V., Grossfield, J. & Pak, W.L. (1972). Phototransduction mutants of *Drosophila melanogaster*. In *Visual System*, ed. Arden, G.B., pp. 1–21. New York: Plenum Press.

Britt, S.G., Feiler, R., Kirschfeld, K. & Zuker, C.S. (1993). Spectral tuning of rhodopsin and metarhodopsin *in vivo*. *Neuron* **11**, 29–39.

Chen, D.M., Brown, G. & Stark, W.S. (1993). Sensitivity and rhabdomere decreases in heterozygotes of *ora*, a nonsense mutant allele of *ninaE*, the *Drosophila* Rh1 opsin gene. *Investigative Ophthalmology and Visual Science* **34**, 808.

Chen, D.M., Christianson, J.S., Brown, G. & Stark, W.S. (1992*a*). Receptor demise from alteration of glycosylation site in *Drosophila* opsin. *Investigative Ophthalmology and Visual Science* **33**, 739.

Chen, D.M., Christianson, J.S., Sapp, R.J. & Stark, W.S. (1992*b*). Visual receptor cycle in normal and *period* mutant *Drosophila*: Microspectrophotometry, electrophysiology, and ultrastructural morphometry. *Visual Neuroscience* **9**, 125–135.

Colley, N.J., Baker, E.K., Stamnes, M.A. & Zuker, C.S. (1991). The cyclophilin homolog *ninaA* is required in the secretory pathway. *Cell* **67**, 255–263.

deCouet, H.G. & Tanimura, T. (1987). Monoclonal antibodies provide evidence that rhodopsin in the outer rhabdomeres of *Drosophila melanogaster* is not glycosylated. *European Journal of Cell Biology* **44**, 50–56.

Dryja, T.P., McGee, T.L., Reichel, E., Hahn, L.B., Cowley, G.S., Yandell, D.W., Sandberg, M.A. & Berson, E.L. (1990). A point mutation of the opsin gene in one form of retinitis pigmentosa. *Nature* (London) **343**, 364–366.

Elbein, A.D. (1987). Inhibitors of the biosynthesis and processing. *Annual Review of Biochemistry* **56**, 497–534.

Fliesler, S.J. & Basinger, S.F. (1985). Tunicamycin blocks the incorporation of opsin into retinal rod outer segment membranes. *Proceedings of the National Academy of Sciences of the U.S.A.* **82**, 1116–1120.

Fliesler, S.J., Rapp, L.M. & Hollyfield, J.G. (1984). Photoreceptor-specific degeneration caused by tunicamycin. *Nature* **311**, 575–577.

Fliesler, S.J., Rayborn, M.E. & Hollyfield, J.G. (1985). Membrane morphogenesis in retinal rod outer segments: Inhibition by tunicamycin. *Journal of Cell Biology* **100**, 574–587.

Harris, W.A. & Stark, W.S. (1977). Hereditary retinal degeneration in *Drosophila melanogaster*. A mutant defect associated with the phototransduction process. *Journal of General Physiology* **69**, 261–291.

Harris, W.A., Stark, W.S. & Walker, J.A. (1976). Genetic dissection of the photoreceptor system in the compound eye of *Drosophila melanogaster*. *Journal of Physiology* (London) **256**, 415–439.

Huber, A., Smith, D.P., Zuker, C.S. & Paulsen, R. (1990). Opsin of *Calliphora* photoreceptors R1-6: homology with *Drosophila* Rh1 and post-translational processing. *Journal of Biological Chemistry* **265**, 17906–17910.

Katz, M.L., Gao, C.L., Kutryb, M., Norberg, N., White, R.H. & Stark, W.S. (1991). Maintenance of opsin density in photoreceptor outer segments of retinoid-deprived rats. *Investigative Ophthalmology and Visual Science* **32**, 1968–1980.

Krishna Prasad, A.V., Plantner, J.J. & Kean, E.L. (1992). Effect of enzymatic deglycosylation on the regenerability of bovine rhodopsin. *Experimental Eye Research* **54**, 913–920.

Leonard, D.S., Bowman, V.D., Ready, D.F. & Pak, W.L. (1992). Degeneration of photoreceptors in rhodopsin mutants of *Drosophila*. *Journal of Neurobiology* **23**, 605–626.

O'Tousa, J.E. (1992). Requirement of N-linked glycosylation site in *Drosophila* rhodopsin. *Visual Neuroscience* **8**, 385–390.

O'Tousa, J.E., Baehr, W., Martin, R.L., Jirsh, J., Pak, W.L. & Applebury, M.L. (1985). The *Drosophila ninaE* gene encodes an opsin. *Cell* **40**, 839–850.

O'Tousa, J.E., Leonard, D.S. & Pak, W.L. (1989). Morphological defects in ora^{JK84} photoreceptors caused by mutation in R1-6 opsin gene in *Drosophila*. *Journal of Neurogenetics* **6**, 41–52.

Ozaki, K., Nagatani, H., Ozaki, M. & Tokunaga, F. (1993). Maturation of major *Drosophila* rhodopsin, *ninaE*, requires chromophore 3-hydroxyretinal. *Neuron* **10**, 1113-1119.

Rosenfeld, P.J., Cowley, G.S., McGee, T.L., Sandberg, M.A., Berson, E.L. & Dryja, T.P. (1992). A *Null* mutation in the rhodopsin gene causes rod photoreceptor dysfunction and autosomal recessive retinitis pigmentosa. *Nature Genetics* **1**, 209–213.

Sapp, R.J., Christianson, J.S., Maier, L., Studer, K. & Stark, W.S. (1991). Carotenoid replacement therapy in *Drosophila*: Recovery of membrane, opsin and rhodopsin. *Experimental Eye Research* **53**, 71–79.

Shaw, S.R. (1981). Anatomy and physiology of identified non-spiking cells in the photoreceptor-lamina complex of the compound eye of insects, especially Diptera. In *Neurons Without Impulses. Society of Experimental Biology Seminar Series 6*, ed. Roberts, A. & Bush, B.M.H., pp. 61–116. Cambridge: University Press.

Stamnes, M.A., Rutherford, S.L. & Zuker, C.S. (1992). Cyclophilins: A new family of proteins involved in intracellular folding. *Trends in Cell Biology* **2**, 272–276.

STARK, W.S., BROWN, G., HOMBS, D., CHRISTIANSON, J.S. & WHITE, R. (1992). Carotenoid replacement in *Drosophila*: Freeze-fracture. *Society for Neuroscience Abstracts* **18**, 1329.

STARK, W.S. & CARLSON, S.D. (1983). Ultrastructure of the compound eye and first optic neuropile of the photoreceptor mutant *ora*^{JK84} of *Drosophila*. *Cell and Tissue Research* **233**, 305–317.

STARK, W.S., CHRISTIANSON, J.S., MAIER, L. & CHEN, D.M. (1991). Inherited and environmentally induced retinal degenerations in *Drosophila*. In *Retinal Degenerations*, ed. ANDERSON, R.E., HOLLYFIELD, J.G. & LAVAIL, M.M., pp. 61–75. New York: CRC Press, Inc.

STARK, W.S. & CLARK, A.W. (1973). Visual synaptic structure in normal and blind *Drosophila*. *Drosophila Information Service* **50**, 105–106.

STARK, W.S., HARTMAN, C.R., SAPP, R.J., CARLSON, S.D., CLAUDE, P. & BHATTACHARYYA, A. (1987). Vitamin A replacement therapy in *Drosophila*. *Drosophila Information Service* **1987**, 136–137.

STARK, W.S., IVANYSHYN, A.M. & GREENBERG, R.M. (1977). Sensitivity and photopigments of R1-6, a two-peaked photoreceptor, in *Drosophila*, *Calliphora* and *Musca*. *Journal Comparative Physiology* **121**, 289–305.

STARK, W.S., IVANYSHYN, A.M. & HU, K.G. (1976). Spectral sensitivities and photopigments in adaptation of fly visual receptors. *Naturwissenschaften* **63**, 513–518.

STARK, W.S. & JOHNSON, M.A. (1980). Microspectrophotometry of *Drosophila* visual pigments: Determinations of conversion efficiency in R1-6 receptors. *Journal of Comparative Physiology* **140**, 275–286.

STARK, W.S. & SAPP, R. (1988). Eye color pigment granules in wild-type and mutant *Drosophila melanogaster*. *Canadian Journal of Zoology* **66**, 1301–1308.

STARK, W.S. & SAPP, R.J. (1987). Ultrastructure of the retina of *Drosophila melanogaster*. The mutant *ora* (*o*uter *r*habdomeres *a*bsent) and its inhibition of degeneration in *rdgB* (*r*etinal *d*egeneration-*B*). *Journal of Neurogenetics* **4**, 227–240.

STARK, W.S. & SAPP, R.J. (1989). Retinal degeneration and photoreceptor maintenance in *Drosophila*: *rdgB* and its interaction with other mutants. In *Inherited and Environmentally Induced Retinal Degenerations*, ed. LAVAIL, M.M., ANDERSON, R.E. & HOLLYFIELD, J.G., pp. 467–489. New York: Liss.

STARK, W.S., SAPP, R.J. & CARLSON, S.D. (1989). Photoreceptor maintenance and degeneration in the *norpA* (*no r*eceptor *p*otential-*A*) mutant of *Drosophila melanogaster*. *Journal of Neurogenetics* **5**, 49–59.

STARK, W.S., SCHILLY, D., CHRISTIANSON, J.S., BONE, R.A. & LANDRUM, J.T. (1990). Photoreceptor-specific efficiencies of β-carotene, zeaxanthin and lutein for photopigment formation deduced from receptor mutant *Drosophila melanogaster*. *Journal of Comparative Physiology* **166**, 429–436.

STARK, W.S. & WASSERMAN, G.S. (1972). Transient and receptor potentials in the electroretinogram of *Drosophila*. *Vision Research* **12**, 1771–1775.

STARK, W.S. & ZITZMANN, W.G. (1976). Isolation of adaptation mechanisms and photopigment spectra by vitamin A deprivation in *Drosophila*. *Journal of Comparative Physiology* **105**, 15–27.

WASHBURN, T. & O'TOUSA, J.E. (1992). Nonsense suppression of the major rhodopsin gene in *Drosophila*. *Genetics* **130**, 585–595.

ZINKL, G., MAIER, L., STUDER, K., SAPP, R., CHEN, D.M. & STARK, W.S. (1990). Microphotometric, ultrastructural and electrophysiological analyses of light-dependent processes on visual receptors in white-eyed wild-type and *norpA* (*no r*eceptor *p*otential) mutant *Drosophila*. *Visual Neuroscience* **5**, 429–439.